TASK-like K^+ channels mediate effects of 5-HT and extracellular pH in rat dorsal vagal neurones *in vitro*

Sarah E. Hopwood[1,2] and Stefan Trapp[1,2]

[1] *Department of Anaesthetics, Pain Medicine and Intensive Care, Division of Surgery, Oncology, Reproductive Biology and* [2] *Biophysics Section, Blackett Laboratory, Imperial College, London, UK*

Dorsal vagal neurones (DVN) receive serotonergic projections from the medullary raphé nuclei, suggesting that 5-HT modulates vagal activity. A previous study has shown that 5-HT excites DVN in part by inhibition of a K^+ current via postsynaptic 5-HT_{2A} receptors. As mRNA for the two-pore-domain K^+ channels TASK-1 (KCNK3) and TASK-3 (KCNK9) has been found in DVN, we investigated the possibility that 5-HT exerts its effects via inhibition of these K^+ channels using whole-cell patch-clamp techniques. In current clamp, 5-HT (20 μM) elicited a depolarization by 5.1 $\pm$ 1.5 mV and an increase in firing rate. In voltage clamp, 5-HT reduced the standing outward current (I_{SO}) at −20 mV by 106 $\pm$ 17 pA, inhibiting a conductance (reversal, −95 $\pm$ 4 mV) which displayed Goldman-Hodgkin-Katz outward rectification, supportive of a TASK-like K^+ current. Since TASK channels are modulated by extracellular pH (pH_o), we next investigated the pH sensitivity of I_{SO} in Hepes-buffered ACSF. At pH_o 7.3, DVN exhibited an I_{SO} of 147 $\pm$ 15 pA at −20 mV. Acidification to pH_o 6.3 reduced I_{SO} to 85 $\pm$ 13 pA, whereas raising pH_o to 8.5 increased I_{SO} to 216 $\pm$ 26 pA. At pH_o 7.3, I_{SO} was inhibited by $BaCl_2$ (IC_{50} 465 μM), but unaffected by $ZnCl_2$ (100 μM). 5-HT (10 μM) reduced I_{SO} by 114 $\pm$ 17 pA at pH_o 7.3, but at pH_o 6.3 the 5-HT-induced inhibition of I_{SO} was significantly smaller. The present data suggest that the excitatory effects of 5-HT on DVN are mediated in part by inhibition of a TASK-like, pH-sensitive K^+ conductance. The pharmacological profile of this conductance excludes TASK-3 homomers, but rather implicates TASK-1-containing channels.

(Resubmitted 20 June 2005; accepted 13 July 2005; first published online 14 July 2005)
Corresponding author S. Trapp: Biophysics Section, Blackett Laboratory, South Kensington Campus, Imperial College London, London SW7 2AZ, UK. Email: s.trapp@imperial.ac.uk

The dorsal motor nucleus of the vagus (DMNX) is the principal source of parasympathetic motor innervation to the subdiaphragmatic viscera, and it plays an integral role in the autonomic control of functions such as gastrointestinal motility, and gastric and pancreatic secretions (Loewy & Spyer, 1990; Powley, 2000). Regulation of the activity of the vagal output neurones is therefore a powerful tool to fine-tune homeostatic processes.

Immunocytochemical studies have shown that the DMNX is densely innervated by 5-hydroxytryptamine (5-HT)-containing terminals (Steinbusch, 1981; Sykes *et al.* 1994). This serotonergic input arises from neurones in the caudal raphé nuclei, including the raphé pallidus and raphé obscurus (Rogers *et al.* 1980), and also from sensory vagal afferents (Sykes *et al.* 1994). In addition, multiple 5-HT receptor subtypes have been identified in the DMNX, including the 5-HT_{2A} receptor present on dorsal vagal neurone (DVN) somata (Wright *et al.* 1995; Fay & Kubin, 2000), as well as the 5-HT_3 (Steward *et al.* 1993) and 5-HT_{1A} subtypes (Thor *et al.* 1992), suggesting that 5-HT exerts fine modulation of vagal activity at the level of the dorsal vagal nucleus.

In fact, previous pharmacological studies *in vitro* have shown that 5-HT increases DVN excitability via direct activation of postsynaptic 5-HT_{2A} receptors (Albert *et al.* 1996; Browning & Travagli, 1999). Similar 5-HT-induced enhancement of excitability is well documented in motoneurones (Rekling *et al.* 2000); for example, Talley *et al.* (2000) have shown that 5-HT depolarizes hypoglossal motoneurones via inhibition of TASK-1 (TWIK-related acid-sensitive K^+ channel-1), a member of the two-pore-domain K^+ channel superfamily.

Two-pore-domain K^+ channels form leak conductances in a variety of tissues, including the CNS. Presently, 15 different human two-pore-domain K^+ channels have been identified and classified into six distinct structural and functional subgroups (Patel & Lazdunski, 2004). They give rise to time- and voltage-independent background K^+ currents, and play a key role in setting neuronal resting membrane potential. Interestingly, these leak conductances are also subject to modulation by

 DOI: 10.1113/jphysiol.2005.093070

intra- and extracellular pH, cell swelling, temperature, volatile anaesthetics, as well as numerous neurotransmitters and modulators (Lesage, 2003). Consequently, their regulation provides a means of fine-tuning neuronal excitability in the face of dynamic environments.

In situ hybridization data indicate that the dorsal vagal nucleus contains mRNA for the acid-sensitive two-pore channels TASK-1 (KCNK3) and TASK-3 (KCNK9), but not TASK-5 (Karschin *et al.* 2001; Talley *et al.* 2001). The present study therefore investigated whether the excitatory effects of 5-HT are mediated by pH-sensitive K^+ currents in DVN. Our results show that 5-HT inhibits a TASK-like K^+ conductance that constitutes a pH-sensitive background current in DVN.

Methods

Slice preparation

Brainstem slices were obtained from 10- to 25-day-old Sprague-Dawley rats in accordance with the Animals (Scientific Procedures) Act 1986. Animals were decapitated under terminal anaesthesia (halothane) and the brainstem was removed. Coronal slices (200 μm thick) were cut around the obex level with a vibratome (Campden Instruments Ltd, Leicester, UK) in ice-cold low-Na^+ artificial cerebrospinal fluid (ACSF) (mM: 2.5 KCl, 200 sucrose, 28 $NaHCO_3$, 1.25 NaH_2PO_4, 3 pyruvate, 7 $MgCl_2$, 0.5 $CaCl_2$, 7 glucose). After cutting, slices were incubated for at least 30 min in modified ACSF at 34°C (mM: 3 KCl, 118 NaCl, 25 $NaHCO_3$, 1.2 NaH_2PO_4, 7 $MgCl_2$, 0.5 $CaCl_2$, 2.5 glucose), and were subsequently maintained at room temperature (RT) in standard ACSF (mM: 3 KCl, 118 NaCl, 25 $NaHCO_3$, 1.2 NaH_2PO_4, 1 $MgCl_2$, 1.5 $CaCl_2$, 10 glucose) until required.

Electrical recordings

Experiments were performed at RT in either standard ACSF or Hepes-buffered ACSF (mM: 3 KCl, 118 NaCl, 1 $MgCl_2$, 1.5 $CaCl_2$, 25 Hepes and 10 glucose; the pH was adjusted to the desired level using NaOH) perfused at a rate of 4–5 ml min^{-1}. Bicarbonate-buffered solutions were gassed continuously with 95% O_2/5% CO_2, and Hepes-buffered ACSF with 100% O_2.

Patch pipettes were pulled from thin-walled borosilicate capillaries (3–6 MΩ; Clark Electromedical Instruments, Pangbourne, UK) with a horizontal puller (Zeitz, Munich, Germany). Electrodes were filled with (mM) 120 potassium gluconate, 1 NaCl, 1 $MgCl_2$, 1 $CaCl_2$, 10 Hepes, 10 BAPTA, 2 K_2ATP, pH 7.3.

Slices were visualized using a ×40 water-immersion lens mounted on an upright microscope fitted with infrared differential interference (DIC) optics (Zeiss, Goettingen, Germany). DVN were identified by their large fusiform shape and anatomical location ventral to the nucleus tractus solitarius (NTS). Cells near to the slice surface were chosen in order to minimize the effect of endogenous pH buffering within the slice (Trapp *et al.* 1996).

Whole-cell recordings were performed in both voltage-clamp and current-clamp mode using an EPC-9 amplifier and Pulse/Pulsefit software (Heka Elektronik, Lambrecht, Germany). Membrane properties were monitored with repetitive 700 ms hyperpolarizing voltage ramps (applied every 20–60 s to allow for full inactivation of the voltage-dependent outward current; see Fig. 2*A*) from a holding potential (V_H) of −20 to −120 mV. Current-clamp recordings were performed in the absence of any holding currents. Membrane potentials or currents were filtered at 1 kHz and digitized at 3 kHz. Compensation for the liquid junction potential (+10 mV) was performed off-line.

Pharmacological agents

Ketanserin tartrate, 5-HT, $BaCl_2$ and $ZnCl_2$ were obtained from Sigma (Poole, UK). All drugs were added directly to the ACSF.

Data analysis

Off-line data analysis was performed using Pulsefit software (Heka). All values are given as means ± S.E.M., where n is number of cells. Statistical comparisons were made using Student's t test with significance accepted at $P < 0.05$. Fitting with the Goldman-Hodgkin-Katz (GHK) current equation was performed with the least-squares method.

For $BaCl_2$ concentration–response relationships, currents at −20 mV were measured in the absence and presence of varying concentrations of $BaCl_2$. Current amplitudes for individual cells were plotted against the $BaCl_2$ concentration, and a mono-exponential function was fitted to the data to approximate the amplitude of the $BaCl_2$-insensitive current component. This current was subtracted from the measured current at all $BaCl_2$ concentrations (0–3 mM). The extent of inhibition of the remaining current (I) by $BaCl_2$ was then expressed as a fraction of the current amplitude (I_c) obtained in the absence of $BaCl_2$. Concentration–response curves were fitted to the Hill equation:

$$I/I_c = 1/\left(1 + ([BaCl_2]/IC_{50})^h\right)$$

where $[BaCl_2]$ is the $BaCl_2$ concentration, IC_{50} is the $BaCl_2$ concentration at which inhibition is half-maximal, and h is the slope factor (Hill coefficient).

Results

5-HT inhibits a K^+ conductance

The effect of 5-HT was initially tested on DVN recorded in current-clamp mode in bicarbonate-buffered ACSF. In agreement with previous studies (Trapp & Ballanyi, 1995), DVN revealed a mean resting potential of -52 ± 2 mV ($n = 12$), and eight of these were spontaneously active, with an action potential firing frequency of 1.6 ± 0.3 Hz. Application of 5-HT (20 μM) for 2 min caused a slow depolarization by 5.1 ± 1.5 mV in 8 of 11 neurones that was accompanied either by an increase in firing rate (Fig. 1*A*) or initiation of firing.

To investigate the nature of the conductances modulated by 5-HT, subsequent experiments were performed under voltage-clamp conditions. DVN were held at -20 mV

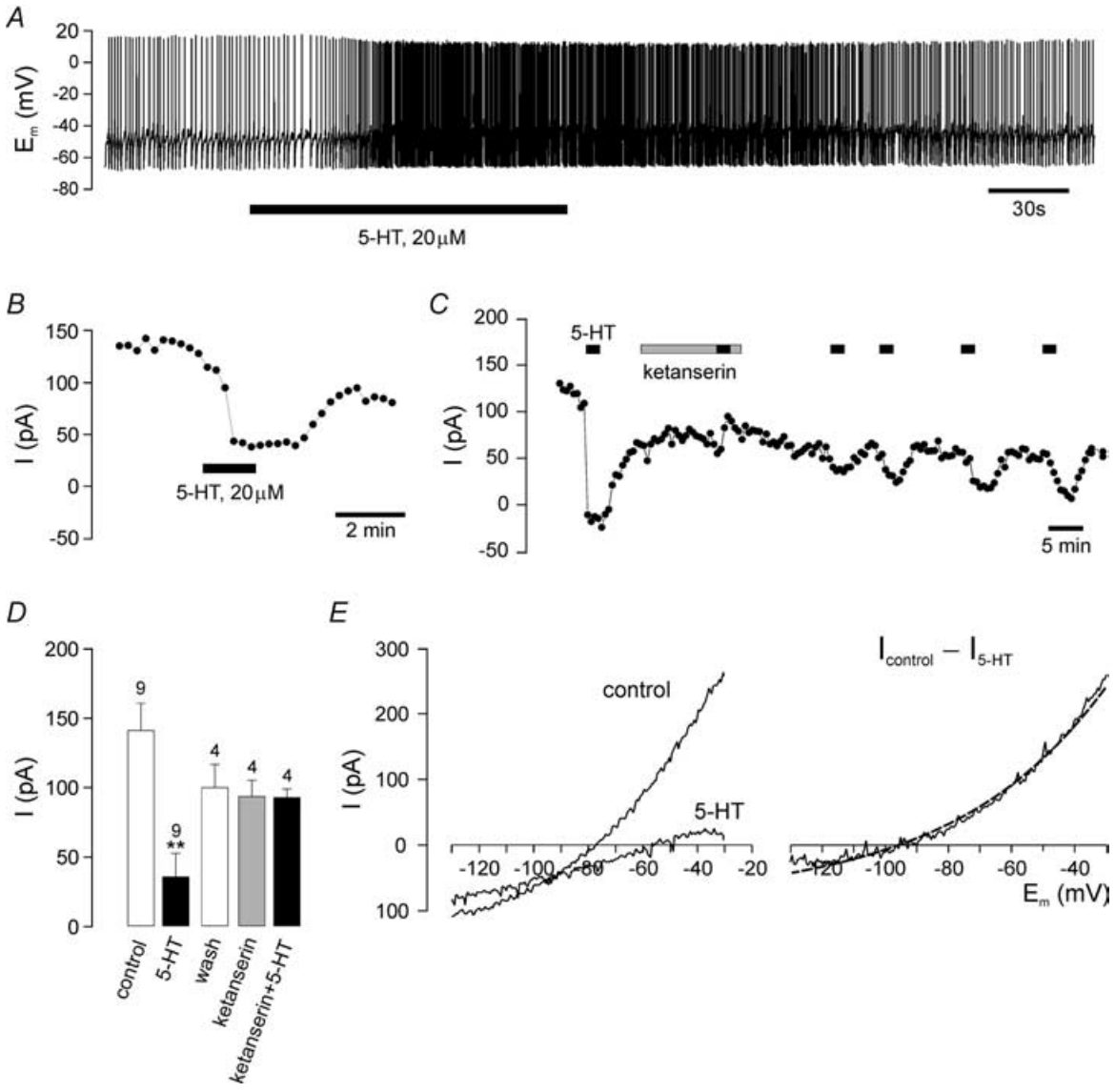

Figure 1. Effects of 5-HT
A, whole-cell current-clamp recording of spontaneous activity of a dorsal vagal neurone (DVN). Bath-application of 5-HT (20 μM) for 2 min (filled bar) causes a reversible, small depolarization and concomitant increase in spontaneous action potential firing. *B*, in voltage clamp, 5-HT reduces the standing outward current (I_{SO}) at -20 mV command voltage. *C*, this effect is completely blocked by prior application of the 5-HT_2 receptor antagonist ketanserin (1 μM). Note the slow recovery of the 5-HT inhibition of I_{SO} after washout of ketanserin, and the rundown of I_{SO} over the course of the recording. *D*, mean effects of 5-HT and ketanserin in recordings similar to those shown in *B* and *C*; 'wash' indicates the current after removal of 5-HT immediately prior to application of ketanserin. The difference between the 'control' and 'wash' bar, which is not statistically significant, reflects the rundown of I_{SO} prior to ketanserin treatment. Number of cells (n) is given above the bars. $^{**}P < 0.01$ *versus* control (unpaired t test). *E*, representative current–voltage relation (*I–V*) obtained from a DVN in the presence and absence of 5-HT (20 μM), and *I–V* for the 5-HT-inhibited current ($I_{control} - I_{5\text{-}HT}$). This current is well described by the Goldman-Hodgkin-Katz (GHK) current equation (dashed line).

to keep voltage-gated conductances inactivated. At this potential the mean whole-cell current was 142 ± 19 pA ($n = 9$). In keeping with previous work (on, for example, cerebellar granule cells; Millar *et al.* 2000), we refer to this resting membrane current at −20 mV as the standing outward current (I_{SO}). Application of 5-HT (20 μM) for 2 min significantly reduced I_{SO} by 106 ± 17 pA ($P < 0.01$, unpaired t test; $n = 9$). Figure 1*B* shows a representative current–time profile for the inhibition of I_{SO} by 5-HT. The effects of 5-HT were completely abolished by prior application of the 5-HT_2 antagonist ketanserin (1 μM) for 10 min (Fig. 1*C* and *D*).

Current–voltage (*I–V*) relations were obtained by applying hyperpolarizing voltage ramps from −20 to −120 mV. Subtraction of *I–V* relationships obtained in the absence and presence of 5-HT (Fig. 1*E*) revealed the 5-HT-sensitive current that reversed at -95 ± 4 mV ($n = 8$), close to the predicted K^+ equilibrium potential (E_K) of −97 mV. Furthermore, the current was well fitted by the GHK equation (Hille, 2001), indicating that 5-HT inhibits an open rectifier K^+ conductance.

Modulation of I_{SO} by extracellular pH

The biophysical properties of the 5-HT-inhibited conductance described above were indicative of a TASK-like current. Both TASK-1 and TASK-3 transcripts are present in the DMNX (Karschin *et al.* 2001; Talley *et al.* 2001), and since a defining hallmark of TASK channels is their sensitivity to changes in extracellular pH, we next investigated the pH sensitivity of I_{SO} in DVN in Hepes-buffered ACSF to enable easy manipulation of extracellular pH.

Figure 2*A* shows the effects of external pH (pH_o) on current responses to the voltage-clamp protocol. At pH_o 7.3, DVN exhibited a mean I_{SO} of 147 ± 15 pA ($n = 17$) at −20 mV, which was not significantly different from that observed in bicarbonate-buffered ACSF. Raising

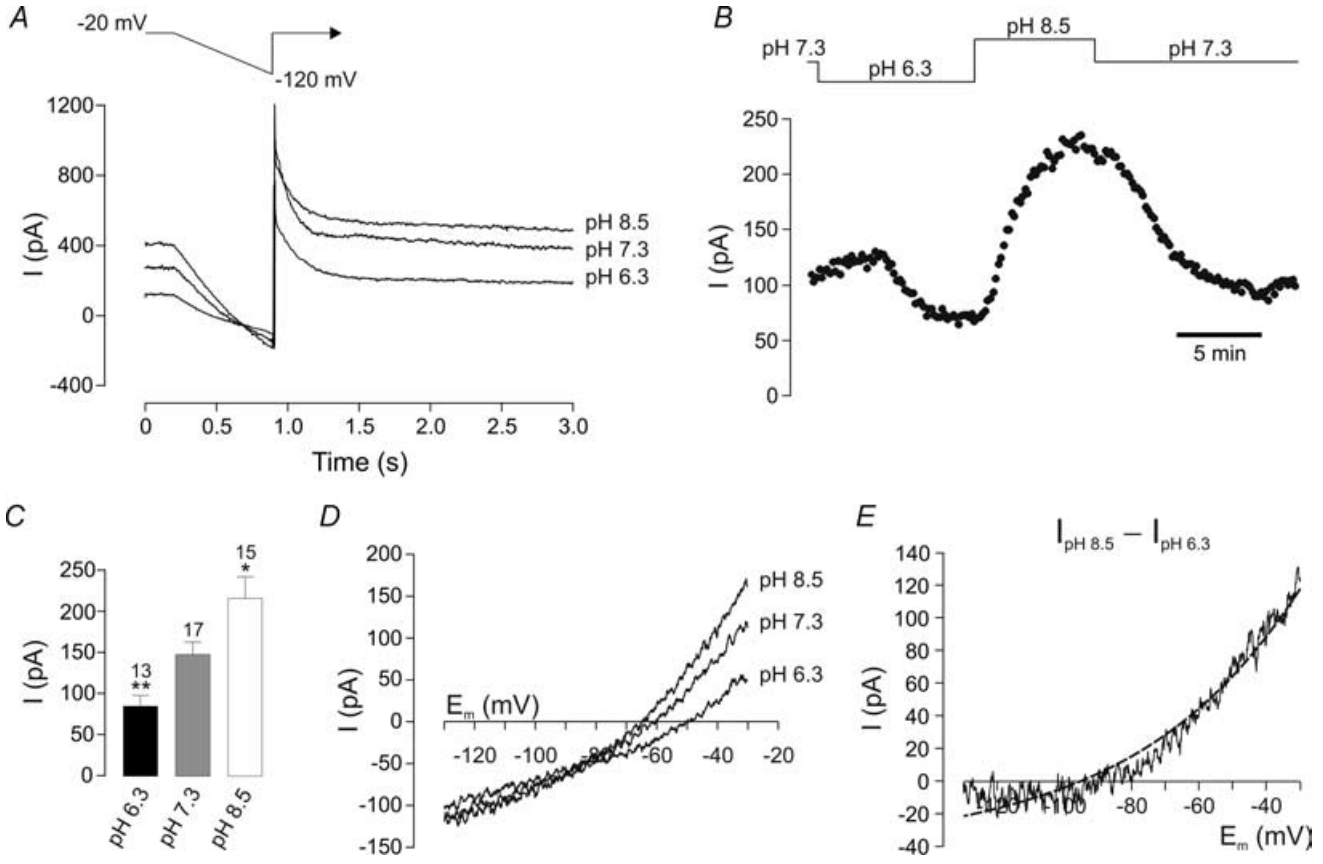

Figure 2. pH dependence of I_{SO}

A, typical traces from a DVN recorded in voltage clamp in Hepes-buffered ACSF at different pH_o values. Acidification (pH_o 6.3) reduces I_{SO} at −20 mV, and alkalinization (pH_o 8.5) increases it. Depolarization from −120 to −20 mV from −120 mV activates a large slowly inactivating outward current. *B*, current amplitude at −20 mV measured over the course of a recording. *C*, mean I_{SO} at different pH values. Number of cells (*n*) is given above the bars. $^*P < 0.05$; $^{**}P < 0.01$ *versus* pH_o 7.3 (unpaired t test). *D*, representative *I–V* relations from a DVN obtained at different pH values. *E*, *I–V* of the acidosis-inhibited current is described by the GHK current equation (dashed line).

the extracellular pH_o from 7.3 to 8.5 was followed by an increase of I_{SO} to 216 ± 26 pA ($n = 15$), whereas acidification to pH_o 6.3 reduced I_{SO} to 85 ± 13 pA ($n = 13$) (Fig. 2*C*). Figure 2*B* shows the time course of a representative experiment. Analysis of the *I–V* relationships (Fig. 2*D*) revealed a corresponding increase and decrease in conductance at pH_o 8.5 and pH_o 6.3, respectively, compared with control conditions (pH_o 7.3), and a reversal potential of the pH-sensitive current near to the predicted value for E_K. *I–V* relationships obtained by subtracting currents evoked at pH_o 6.3 from those at pH_o 8.5 yielded a conductance that displayed GHK open rectification (Fig. 2*E*), and was thus very similar to the 5-HT-sensitive current. In a further four cells, increasing pH_o from 8.5 to 9.2 actually decreased I_{SO} at −20 mV by 36 ± 5 pA.

Pharmacological profile of I_{SO}

Relatively few pharmacological agents are able to discriminate between TASK-1 and TASK-3, although TASK-1 is more sensitive to blockade by external Ba^{2+} (IC_{50} values: rat TASK-1, 0.35 mM; rat TASK-3, 3 mM) (Kim *et al.* 2000; Millar *et al.* 2000). TASK-3 is characteristically blocked by low concentrations of external Zn^{2+} (IC_{50}: human TASK-3, 20 μM), whereas human and rat TASK-1 are virtually Zn^{2+} insensitive (Clarke *et al.* 2004). Here we exploited these properties to investigate the relative contribution of TASK-1 and/or TASK-3 to I_{SO} in DVN.

When I_{SO} was maximized by increasing extracellular pH_o to 8.5, $BaCl_2$ (1 mM) significantly inhibited the current at −20 mV by 131 ± 39 pA ($P < 0.05$, paired *t* test; $n = 6$) (Fig. 3*A* and *B*). Furthermore, at pH_o 7.3, $BaCl_2$ produced a concentration-dependent inhibition of I_{SO} at −20 mV (IC_{50} 465 μM; Fig. 3*C*), suggesting that TASK-1 channels contribute to I_{SO}.

As well as TASK, Ba^{2+} is known to block inward rectifier K^+ (Kir) channels (albeit with much higher affinity), which are present in some DVN (Travagli & Gillis, 1994). Indeed, application of 30 μM Ba^{2+} for 3 min inhibited an inwardly rectifying current (Fig. 4*A*, and lower panel in Fig. 4*C*), increasing I_{SO} at V_H −120 mV by 44 ± 14 pA ($P < 0.05$, paired *t* test; $n = 5$), but did not significantly affect I_{SO} at −20 mV (Fig. 4*B*). Subsequent addition of 1 mM Ba^{2+} had no further significant effect on I_{SO} at −120 mV, but reduced I_{SO} at −20 mV by 67 ± 19 pA ($P < 0.05$, paired *t* test; $n = 5$). Subtraction of *I–V* relations obtained during 1 mM Ba^{2+} from those during 30 μM Ba^{2+} revealed a conductance that displayed properties consistent with an openly rectifying K^+ channel, as illustrated in Fig. 4*C* (upper panel).

Figure 5*A* and *B* shows that at pH_o 7.3, application of $ZnCl_2$ (100 μM) had no effect on I_{SO} at −20 mV ($n = 4$), despite I_{SO} being inhibited by extracellular acidification. Taken together, these results suggest that TASK-1

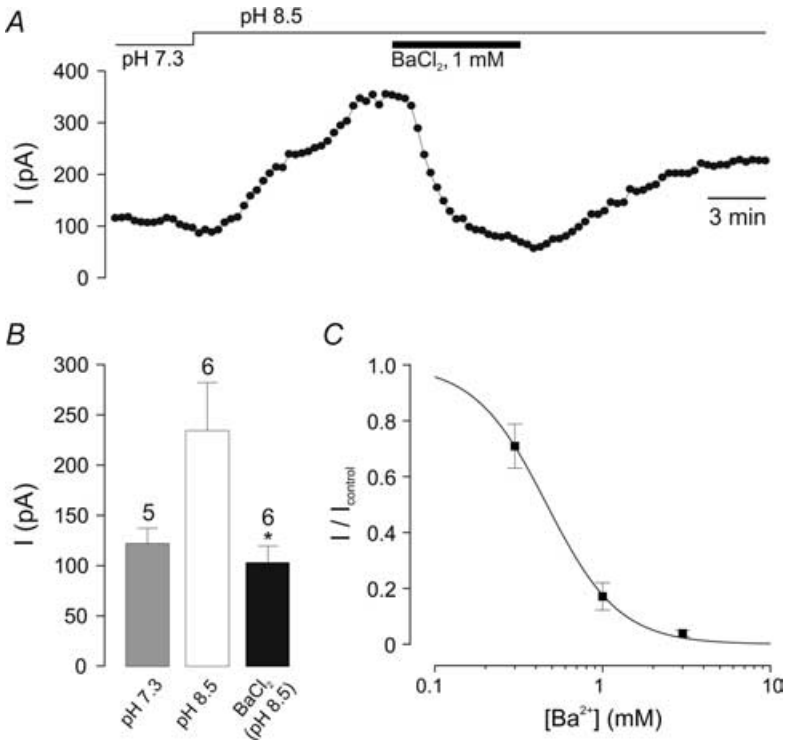

Figure 3. $BaCl_2$ sensitivity of the TASK-like current
A, the alkalinization-activated I_{SO} at −20 mV is inhibited by 1 mM $BaCl_2$. This effect is partially reversible. *B*, mean data from recordings as shown in *A*. Number of cells (*n*) are given above the bars. $^*P < 0.05$ *versus* pH_o 8.5 (unpaired *t* test). *C*, concentration–response curve for $BaCl_2$ at pH_o 7.3. $I/I_{control}$ is the current in the presence of $BaCl_2$ expressed as a fraction of the current prior to $BaCl_2$ application. The line is the best fit to the Hill equation using an IC_{50} of 465 ± 11 μM and Hill coefficient of 2.01 ± 0.08.

rather than TASK-3 channels mediate the pH-sensitive current.

Extracellular acidification occludes the response to 5-HT

Finally, in order to ascertain that the 5-HT-inhibited and acid-sensitive K^+ currents were mediated by the same channels, we compared the effects of 5-HT (10 μM) under control conditions (pH_o 7.3) and at pH_o 6.3. A representative recording is shown in Fig. 6*A*. At pH_o 7.3, 5-HT (10 μM) reduced I_{SO} by 114 ± 17 pA ($n = 6$), whereas at pH_o 6.3, the 5-HT-induced reduction in I_{SO} was significantly smaller ($P < 0.01$, paired t test; $n = 6$) (Fig. 6*B*), indicating that at least a significant proportion of the current inhibited by 5-HT is sensitive to extracellular acidosis. Analysis of the *I–V* relationship of the 5-HT-inhibited current at pH 6.3 revealed an inward current over the entire voltage range in two cells, and a reversal potential near E_K in four recordings. However, the small amplitude of these currents prevented meaningful analysis of the rectification properties of the K^+ currents.

Discussion

Our results provide evidence that 5-HT modulates a TASK-like K^+ channel in DVN. Albert *et al.* (1996) previously attributed the excitatory effect of 5-HT on DVN to stimulation of postsynaptic 5-HT_{2A} receptors, and speculated that '5-HT, in part, closes K^+ leak channels'. In the present study we provide evidence that this then elusive 'leak' current is mediated by TASK channels. Specifically, we demonstrated that 5-HT_2 receptor activation reduced I_{SO} in DVN by inhibiting an

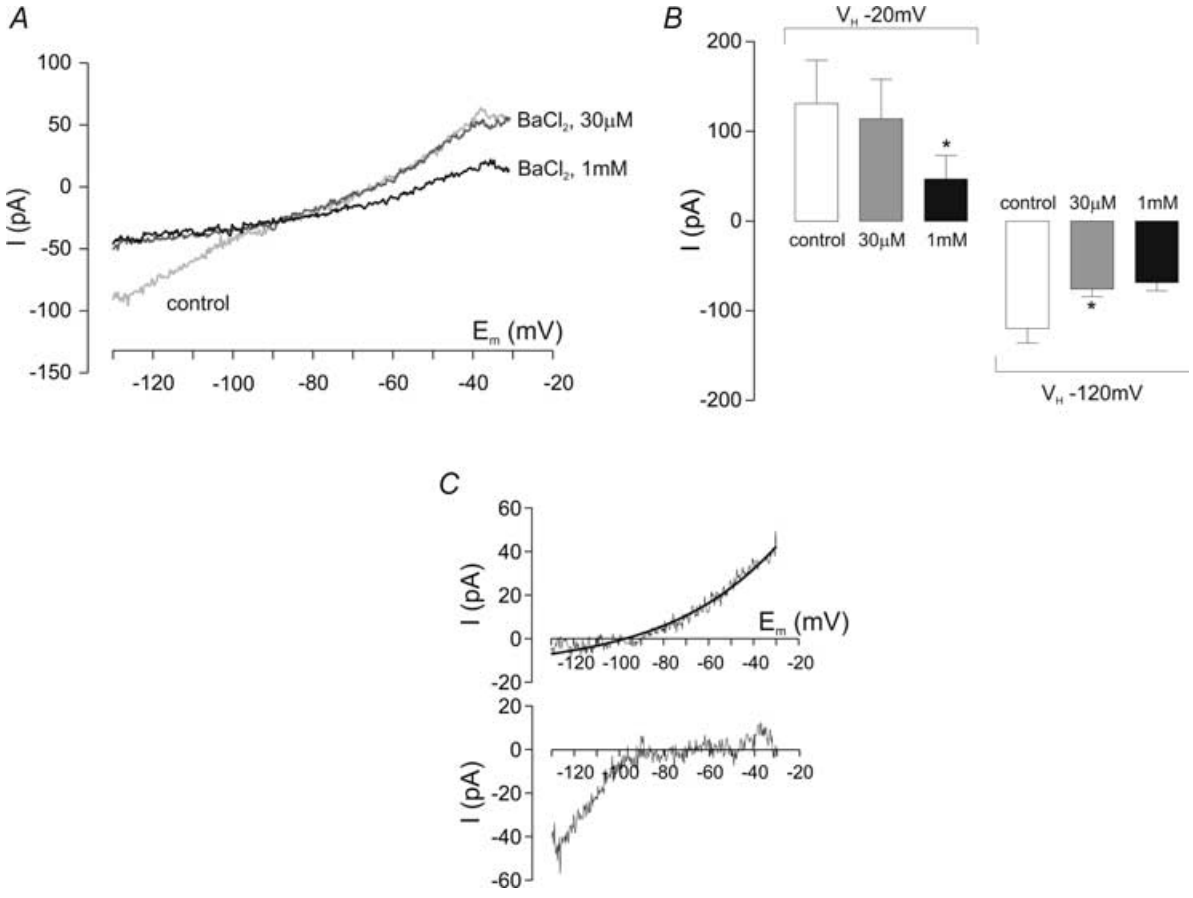

Figure 4. $BaCl_2$ inhibition of both Kir and TASK-like currents
A, a low concentration (30 μM) of $BaCl_2$ inhibits primarily an inward K^+ current in DVN. Increasing $BaCl_2$ to 1 mM inhibited mainly an outward current. *B*, mean current amplitude at a command potential of −20 and −120 mV in the absence and presence of 30 μM or 1 mM $BaCl_2$, respectively (all bars $n = 5$). $^*P < 0.05$ *versus* 30 μM $BaCl_2$ at holding potential (V_H) −20 mV; $^*P < 0.05$ *versus* control at V_H −120 mV (paired t test). *C*, lower panel, *I–V* relation of current inhibited by 30 μM $BaCl_2$, indicative of a strongly rectifying Kir channel; upper panel, *I–V* relation of current inhibited by the increase of $BaCl_2$ from 30 μM to 1 mM. This current is described well by the GHK current equation (continuous line).

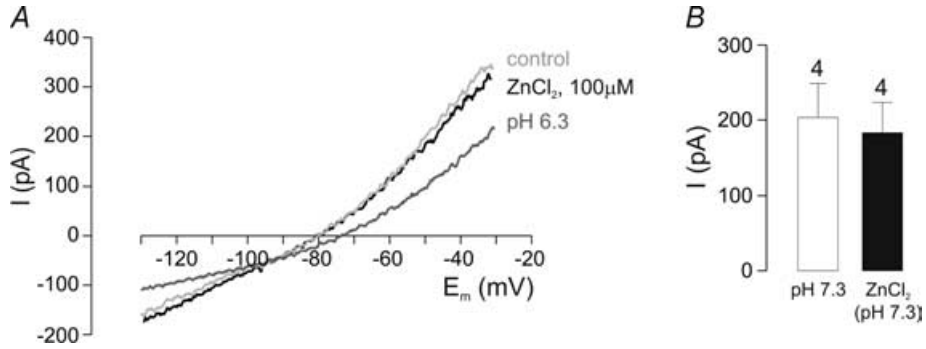

Figure 5. Effects of $ZnCl_2$
A, *I–V* relations at pH_o 7.3 in the presence and absence of 100 μM $ZnCl_2$, and at pH_o 6.3. The TASK-3 blocker $ZnCl_2$ failed to inhibit the pH-sensitive K^+ current. *B*, mean data from recordings as shown in *A*. Number of cells (*n*) is given above the bars.

openly rectifying conductance that reversed near to E_K. Furthermore, the 5-HT-modulated current was markedly attenuated by extracellular acidification. The sensitivity of I_{SO} to changes in pH_o further supported a functional role for TASK channels in DVN: specifically, I_{SO} was augmented and inhibited by extracellular alkalization and acidification, respectively.

Like TASK channels, some inwardly rectifying K^+ (Kir) channels can be modulated by pH and G-protein-coupled receptors. However, the only Kir channel known to be inhibited by extracellular acidification is Kir2.3 (Coulter *et al.* 1995). DVN have recently been shown to express moderate levels of Kir4.1 and Kir5.1, but very little Kir1.1 or Kir2.3 transcript (Wu *et al.* 2004). In agreement with our results, Travagli & Gillis (1994) observed that a proportion of rat DVN exhibit strongly rectifying Kir-type currents. In the present study, we used a low concentration of Ba^{2+} as a tool to block these Kir channels, thereby unmasking the TASK-like K^+ conductance. Moreover, the fact that 5-HT clearly inhibited an open rectifier precludes the involvement of a Kir-type conductance in the effects of 5-HT. This confirms the finding by Browning & Travagli (1999) that 5-HT (30 μM) did not affect the amplitude of Kir currents in DVN.

In DVN, most of the 5-HT-sensitive K^+ current appears to be carried through TASK channels, as indicated by the attenuation of the 5-HT response by lowering extracellular pH. However, the response to the neurotransmitter was larger than that induced by extracellular acidification. This finding could indicate that not all TASK channels were blocked at pH 6.3; thus, any residual effect of 5-HT would be abolished by further reducing extracellular pH, although this was not tested (but see Patel & Honore, 2001: rat TASK-1 is 95% inhibited at pH_o 6.4). Alternatively the residual effect of 5-HT may be attributed to an effect on other conductances. For example, in trigeminal motoneurones, as well as reducing a leak K^+ current, 5-HT enhances the hyperpolarization-activated cationic current (I_h) and also induces a Na^+-dependent inward current (Hsiao *et al.* 1997). Our results do not rule out any of these

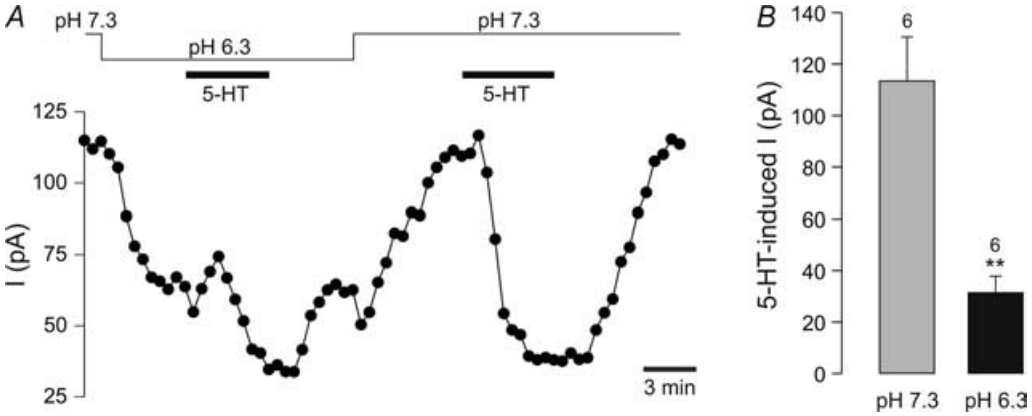

Figure 6. Dependence of 5-HT effects on extracellular pH
A, modulation of I_{SO} at −20 mV in response to 5-HT at pH_o 6.3 and at pH_o 7.3. I_{SO} was measured every 30 s. *B*, mean inhibition of I_{SO} by 5-HT at the pH indicated. The number of cells (*n*) is given above the bars. ** $P < 0.01$ *versus* control (pH_o 7.3) (paired *t* test).

possibilities, but do suggest that in some cells the entire 5-HT-sensitive K^+ current can be blocked by pH 6.3.

pH sensitivity: TASK-1 *versus* TASK-3

Our results suggest that TASK-1 channels underlie a major component of I_{SO} in DVN. Both TASK-1 and TASK-3 are activated by alkalization and inhibited by acidification, although the sensitivity of TASK-1 centres on physiological pH (pK_a ∼7.4), whereas the pK_a for TASK-3 lies more in the acidified range (pK_a ∼6.7) (Talley *et al.* 2003). Accordingly, at pH_o 7.3, TASK-3 currents are almost fully activated (Kim *et al.* 2000). However, for the majority of DVN, raising extracellular pH_o from 7.3 to 8.5 led to an increase in I_{SO} and membrane conductance, suggesting activation of TASK-1 (and not TASK-3). This is further supported by the finding that I_{SO} is insensitive to blockade by the TASK-3 channel blocker Zn^{2+} (100 μM $ZnCl_2$ inhibits both mouse and human TASK-3 expressed in HEK 293 cells by >80%; Alistair Mathie, personal communication) yet is blocked by Ba^{2+}, with an IC_{50} value similar to that obtained for rat TASK-1 expressed in oocytes.

There is increasing evidence to suggest that TASK-1 and TASK-3 can coassociate into functional heteromeric channels *in vivo* (Berg *et al.* 2004; Kang *et al.* 2004). The DMNX contains a high density of TASK-1 and TASK-3 mRNA, and it is possible that these channels are coexpressed in DVN. K^+ currents through heteromeric TASK-1/TASK-3 channels display intermediate pH_o sensitivity (Czirjak & Enyedi, 2002; Berg *et al.* 2004) and are relatively insensitive to blockade by Zn^{2+} compared with TASK-3 homodimers (Clarke *et al.* 2004). The results from the present study therefore cannot exclude a possible contribution of heteromeric TASK-1/TASK-3 channels to I_{SO} in DVN.

Interestingly, DVN exhibit a more depolarized resting membrane potential (RMP) (-52 ± 2 mV; this study) compared with other neuronal populations expressing TASK-like currents, such as cerebellar granule cells (*in vitro* RMP -78 ± 4 mV; Clarke *et al.* 2004). The standing outward K^+ current (termed IK_{SO}) responsible for the large negative RMP in these cells was initially attributed to TASK-1 (Millar *et al.* 2000), although a recent study indicates that TASK-3 homodimers constitute a major component of IK_{SO} (Clarke *et al.* 2004). If, as the current results suggest, the pH-sensitive background current in DVN is carried primarily via TASK-1 (and not TASK-3) channels, the fact that TASK-1 channels would only be 50% activated at physiological pH might contribute to the more depolarized nature of DVN compared with neurones expressing TASK-3 currents.

The TASK-2 channel (Reyes *et al.* 1998; Gray *et al.* 2000) is functionally similar to TASK-1 and TASK-3 in that it mediates a noninactivating, outwardly rectifying K^+ current that is highly sensitive to pH_o (pK_a ∼7.6). Despite reports of insignificant mRNA expression in the rat CNS (with the exception of the spinal cord) by *in situ* hybridization (Talley *et al.* 2001) or RT-PCR analysis (Gray *et al.* 2000), an immunohistochemical study (Gabriel *et al.* 2002) has localized TASK-2 immunoreactivity to a number of rat brain regions, including the DMNX. In addition, one functional study has identified TASK-2 as a component of IK_{SO} in cultured rat cerebellar granule cells. TASK-2 (like the other two alkalosis-activated two-pore K^+ channels TALK-1 and TALK-2) displays sensitivity over a much wider range of alkaline pH_o levels than TASK-1; indeed, Kang & Kim (2004) found that raising the external pH from 8.3 to 10.3 markedly increased whole-cell currents in COS-7 cells expressing TASK-2. In contrast, TASK-1 is almost fully activated at pH levels above 8.5 (Duprat *et al.* 1997; Talley *et al.* 2000), and similarly, we found that increasing extracellular pH from 8.5 to 9.2 actually slightly reduced I_{SO} at -20 mV in DVN.

Functional implications of TASK channel modulation

The physiological relevance of the pH sensitivity of DVN remains to be established. Central chemoreception is located primarily within the lower brainstem and particularly the ventrolateral medulla (VLM) has been implicated in the effects of hypercapnia and acidosis on central respiratory drive (for reviews see Ballantyne & Scheid, 2001; Feldman *et al.* 2003). Recently it has been proposed that the chemosensors are specialized cells, located in the retrotrapezoid nucleus, which innervate key respiratory centres, and that expression of two-pore-domain K^+ channels in these neurones confers chemosensitivity (Mulkey *et al.* 2004). By way of analogy, Coates *et al.* (1993) demonstrated that local acidification of the NTS/DMNX area in the dorsal brainstem (induced by pressure injection of acetazolamide) led to an increase in phrenic nerve activity and/or blood pressure in the anaesthetized cat and rat, suggesting that central chemosensitivity for cardiovascular regulation might reside in this area. The presence of individual chemosensitive neurones within the NTS and DMNX was later confirmed in an *in vitro* study (Huang *et al.* 1997). Our results would suggest that like in the VLM, chemosensitivity in the DMNX is mediated by two-pore-domain K^+ channels, or more specifically, TASK-like channels. Given the strong activation of TASK-1 channels by volatile anaesthetics, this would suggest that (for example) halothane-induced anaesthesia might cause a reduced responsiveness to challenges such as respiratory acidosis. It would also be of considerable interest to investigate whether ablation of TASK-1 in transgenic animals abolishes or diminishes central chemoreception. In this context it should be noted that DVN are the 'output' cells of the vagal system. Consequently their intrinsic chemosensitivity

would modulate the activity of the efferent vagal nerve independent of signals from chemosensitive sites further upstream.

In agreement with earlier work (Albert *et al.* 1996; Browning & Travagli, 1999), a large proportion of DVN responded to 5-HT with an increase in electrical activity. This might suggest that 5-HT arising from caudal raphé neurones acts on TASK-like background channels to modulate DVN excitability and vagal tone in concert with other parameters, such as extracellular pH, in order to fine-tune vagal output in relation to a dynamic environment, as well as different behavioural states or general arousal. Furthermore, it seems feasible to postulate that functional TASK channels in DVN might be the substrate for regulation of vagal tone by volatile anaesthetics as well as by a number of other neuromodulators and neurotransmitters that have been shown to affect K^+ currents.

References

Albert AP, Spyer KM & Brooks PA (1996). The effect of 5-HT and selective 5-HT receptor agonists and antagonists on rat dorsal vagal preganglionic neurones *in vitro*. *Br J Pharmacol* **119**, 519–526.

Ballantyne D & Scheid P (2001). Central chemosensitivity of respiration: a brief overview. *Respir Physiol* **129**, 5–12.

Berg AP, Talley EM, Manger JP & Bayliss DA (2004). Motoneurons express heteromeric TWIK-related acid-sensitive K^+ (TASK) channels containing TASK-1 (KCNK3) and TASK-3 (KCNK9) subunits. *J Neurosci* **24**, 6693–6702.

Browning KN & Travagli RA (1999). Characterization of the *in vitro* effects of 5-hydroxytryptamine (5-HT) on identified neurones of the rat dorsal motor nucleus of the vagus (DMV). *Br J Pharmacol* **128**, 1307–1315.

Clarke CE, Veale EL, Green PJ, Meadows HJ & Mathie A (2004). Selective block of the human 2-P domain potassium channel, TASK-3, and the native leak potassium current, IK_{SO}, by zinc. *J Physiol* **560**, 51–62.

Coates EL, Li A & Nattie EE (1993). Widespread sites of brain stem ventilatory chemoreceptors. *J Appl Physiol* **75**, 5–14.

Coulter KL, Perier F, Radeke CM & Vandenberg CA (1995). Identification and molecular localization of a pH-sensing domain for the inward rectifier potassium channel HIR. *Neuron* **15**, 1157–1168.

Czirjak G & Enyedi P (2002). Formation of functional heterodimers between the TASK-1 and TASK-3 two-pore domain potassium channel subunits. *J Biol Chem* **277**, 5426–5432.

Duprat F, Lesage F, Fink M, Reyes R, Heurteaux C & Lazdunski M (1997). TASK, a human background K^+ channel to sense external pH variations near physiological pH. *EMBO J* **16**, 5464–5471.

Fay R & Kubin L (2000). Pontomedullary distribution of $5\text{-}HT_{2A}$ receptor-like protein in the rat. *J Comp Neurol* **418**, 323–345.

Feldman JL, Mitchell GS & Nattie EE (2003). Breathing: rhythmicity, plasticity, chemosensitivity. *Annu Rev Neurosci* **26**, 239–266.

Gabriel A, Abdallah M, Yost CS, Winegar BD & Kindler CH (2002). Localization of the tandem pore domain K^+ channel KCNK5 (TASK-2) in the rat central nervous system. *Brain Res Mol Brain Res* **98**, 153–163.

Gray AT, Zhao BB, Kindler CH, Winegar BD, Mazurek MJ, Xu J, Chavez RA, Forsayeth JR & Yost CS (2000). Volatile anesthetics activate the human tandem pore domain baseline K^+ channel KCNK5. *Anesthesiology* **92**, 1722–1730.

Hille B (2001). *Ion Channels of Excitable Membranes*. Sinauer Associates, Sunderland.

Hsiao CF, Trueblood PR, Levine MS & Chandler SH (1997). Multiple effects of serotonin on membrane properties of trigeminal motoneurons *in vitro*. *J Neurophysiol* **77**, 2910–2924.

Huang RQ, Erlichman JS & Dean JB (1997). Cell–cell coupling between CO_2-excited neurons in the dorsal medulla oblongata. *Neuroscience* **80**, 41–57.

Kang D, Han J, Talley EM, Bayliss DA & Kim D (2004). Functional expression of TASK-1/TASK-3 heteromers in cerebellar granule cells. *J Physiol* **554**, 64–77.

Kang D & Kim D (2004). Single-channel properties and pH sensitivity of two-pore domain K^+ channels of the TALK family. *Biochem Biophys Res Commun* **315**, 836–844.

Karschin C, Wischmeyer E, Preisig-Muller R, Rajan S, Derst C, Grzeschik KH, Daut J & Karschin A (2001). Expression pattern in brain of TASK-1, TASK-3, and a tandem pore domain K^+ channel subunit, TASK-5, associated with the central auditory nervous system. *Mol Cell Neurosci* **18**, 632–648.

Kim Y, Bang H & Kim D (2000). TASK-3, a new member of the tandem pore K^+ channel family. *J Biol Chem* **275**, 9340–9347.

Lesage F (2003). Pharmacology of neuronal background potassium channels. *Neuropharmacology* **44**, 1–7.

Loewy AD & Spyer KM (1990). Vagal preganlionic neurons. *Central Regulation of Autonomic Functions*, pp. 68–67. Oxford University Press, New York.

Millar JA, Barratt L, Southan AP, Page KM, Fyffe RE, Robertson B & Mathie A (2000). A functional role for the two-pore domain potassium channel TASK-1 in cerebellar granule neurons. *Proc Natl Acad Sci U S A* **97**, 3614–3618.

Mulkey DK, Stornetta RL, Weston MC, Simmons JR, Parker A, Bayliss DA & Guyenet PG (2004). Respiratory control by ventral surface chemoreceptor neurons in rats. *Nat Neurosci* **7**, 1360–1369.

Patel AJ & Horne E (2001). Properties and modulation of mammalian 2P domain K^+ channels. *Trends Neurosci* **24**, 339–346.

Patel AJ & Lazdunski M (2004). The 2P-domain K^+ channels: role in apoptosis and tumorigenesis. *Pflugers Arch* **448**, 261–273.

Powley TL (2000). Vagal circuitry mediating cephalic-phase responses to food. *Appetite* **34**, 184–188.

Rekling JC, Funk GD, Bayliss DA, Dong XW & Feldman JL (2000). Synaptic control of motoneuronal excitability. *Physiol Rev* **80**, 767–852.

Reyes R, Duprat F, Lesage F, Fink M, Salinas M, Farman N & Lazdunski M (1998). Cloning and expression of a novel pH-sensitive two-pore domain K^+ channel from human kidney. *J Biol Chem* **273**, 30863–30869.

Rogers RC, Kita H, Butcher LL & Novin D (1980). Afferent projections to the dorsal motor nucleus of the vagus. *Brain Res Bull* **5**, 365–373.

Steinbusch HW (1981). Distribution of serotonin-immunoreactivity in the central nervous system of the rat-cell bodies and terminals. *Neuroscience* **6**, 557–618.

Steward LJ, West KE, Kilpatrick GJ & Barnes NM (1993). Labelling of 5-HT_3 receptor recognition sites in the rat brain using the agonist radioligand [^{3}H]meta-chlorophenylbiguanide. *Eur J Pharmacol* **243**, 13–18.

Sykes RM, Spyer KM & Izzo PN (1994). Central distribution of substance P, calcitonin gene-related peptide and 5-hydroxytryptamine in vagal sensory afferents in the rat dorsal medulla. *Neuroscience* **59**, 195–210.

Talley EM, Lei Q, Sirois JE & Bayliss DA (2000). TASK-1, a two-pore domain K^+ channel, is modulated by multiple neurotransmitters in motoneurons. *Neuron* **25**, 399–410.

Talley EM, Sirois JE, Lei Q & Bayliss DA (2003). Two-pore-domain (KCNK) potassium channels: dynamic roles in neuronal function. *Neuroscientist* **9**, 46–56.

Talley EM, Solorzano G, Lei Q, Kim D & Bayliss DA (2001). CNS distribution of members of the two-pore-domain (KCNK) potassium channel family. *J Neurosci* **21**, 7491–7505.

Thor KB, Blitz-Siebert A & Helke CJ (1992). Autoradiographic localization of 5-HT_1 binding sites in the medulla oblongata of the rat. *Synapse* **10**, 185–205.

Trapp S & Ballanyi K (1995). KATP channel mediation of anoxia-induced outward current in rat dorsal vagal neurons in vitro. *J Physiol* **487**, 37–50.

Trapp S, Luckermann M, Brooks PA & Ballanyi K (1996). Acidosis of rat dorsal vagal neurons *in situ* during spontaneous and evoked activity. *J Physiol* **496**, 695–710.

Travagli RA & Gillis RA (1994). Hyperpolarization-activated currents, I_H and I_{KIR}, in rat dorsal motor nucleus of the vagus neurons *in vitro*. *J Neurophysiol* **71**, 1308–1317.

Wright DE, Seroogy KB, Lundgren KH, Davis BM & Jennes L (1995). Comparative localization of serotonin 1A, 1C, and 2 receptor subtype mRNAs in rat brain. *J Comp Neurol* **351**, 357–373.

Wu J, Xu H, Shen W & Jiang C (2004). Expression and coexpression of CO_2-sensitive Kir channels in brainstem neurons of rats. *J Membr Biol* **197**, 179–191.

Acknowledgements

We thank Alistair Mathie for valuable discussions and critical comments. This work was supported by a Career Development Award to S.T. from the MRC.